179th Meeting of the Acoustical Society of America

Acoustics Virtually Everywhere

7-11 December 2020

Computational Acoustics: Paper 2aCAa4

Simulations and case study of X-59 low-booms propagated through measured atmospheric profiles

William Jeffrey Doebler
Structural Acoustics Branch, NASA Langley Research Center, Hampton, VA, 23517;
william.j.doebler@nasa.gov

NASA's X-59 Quiet Supersonic Technology aircraft will soon be used to collect data to support the development of a dose-response relationship between low-boom level and human perception. The X-59's low-boom level will depend on aircraft conditions and trajectory, which can be controlled, and on atmospheric conditions, which cannot be controlled. To assess variability in low-boom levels produced by realistic atmospheres, NASA's PCBoom code was used to simulate propagation of an X-59 nearfield pressure condition through atmospheric profiles measured during NASA's Quiet Supersonic Flights 2018 (QSF18) test. Despite QSF18 lasting only 11 days, substantial weather variability occurred including snow and record high temperatures. A PL range of about 8.5 dB was predicted due to the QSF18 atmospheric variability. These results demonstrate the necessity for X-59's flight condition to be adjusted based on atmospheric conditions in order to achieve desired loudness levels during community surveys. Undertrack booms' Perceived Levels (PL) were predicted not to exceed 75 dB, X-59's target level in a standard atmosphere. Attenuation rate, ray tube area, path length and other quantities are presented throughout propagation for the atmospheres that produce the loudest and quietest booms. Humidity differences below 15kft were a primary driver of the PL differences.

1. BACKGROUND

NASA will soon be conducting community noise surveys using the X-59 Quiet Supersonic Technology aircraft that is currently under construction.[1] This aircraft has been designed to produce a shaped sonic boom, also known as a low-boom or sonic thump, of 75 dB on the Stevens Perceived Level (PL) scale.[2,3] The loudness of the X-59 sonic thump at the ground is impacted by variability in the atmospheric profile along its propagation path. This variability in PL due only to the macroscopic atmospheric effects illustrates a challenge for planning X-59 low-boom community noise surveys.

Previous X-59 sonic boom propagation simulation studies have used atmospheric profiles produced by weather models as inputs to investigate seasonal and geographical variability carpet width and sonic boom perception metrics at the ground due to macroscopic atmospheric effects.[4] These propagation simulations utilized atmospheric profiles with coarser vertical resolution than those typically used for NASA post-flight sonic boom propagation analysis using weather balloon measurements. Propagation simulations utilizing measured weather balloon profiles can complement the simulations from weather models. In this paper, the X-59 sonic boom was propagated through twenty-two atmospheric profiles measured by weather balloons during the NASA's Quiet Supersonic Flights 2018 (QSF18) test.[5]

QSF18 was a community noise survey and flight test during which an F-18 aircraft performed a supersonic dive maneuver[6] that produces low-amplitude sonic booms. The test was conducted in Galveston, TX and lasted for eleven days. Twenty-two F-18 flights were completed, with one to three supersonic dives per flight, for a total of fifty-two low-amplitude sonic booms. Prior to each flight, a weather balloon was launched to gather atmospheric profile data (pressure, temperature, wind speed and direction, and humidity). Substantial surface weather variability was observed during this brief test, including both record high temperatures with heat advisories as well as record low temperatures with light snowfall. The variability of the measured atmospheric profiles makes them interesting candidates for analyzing X-59's low-boom performance.

This work examines predictions of X-59 low-boom levels and carpet widths resulting from atmospheric profile measurements that were collected during QSF18. It also includes an in-depth case study of the two X-59 booms that were predicted to have the greatest difference in PL at the ground.

2. PROPAGATION SIMULATIONS

A. PROPAGATION DESCRIPTION

The X-59 C609 nearfield pressure data in its design condition (steady cruise at Mach 1.4 at 54,000 ft (16459.2 m)) generated using FUN3D with two degree azimuthal resolution is shown in Figure 1 for four selected azimuthal angles.[7] The nearfield pressure was propagated through the atmospheric profiles measured by weather balloons during the QSF18 test from aircraft to ground using PCBoom 6.7.1.[8,9]
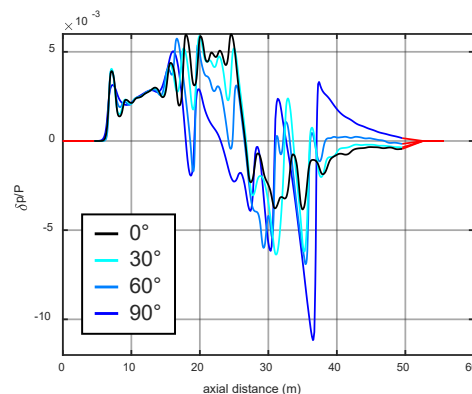

Figure 1. Nearfield pressure data for the X-59 C609. δp is the acoustic pressure, and P is the free-stream pressure. The black line is the undertrack (0°) nearfield signature. The 30°, 60°, and 90° azimuthal waveforms are also shown. The aircraft nearfield is azimuthally symmetric. The portions of red on the waveforms are post-processed extensions so that the waveform returns smoothly to δp/P=0.

The PCBoom 6.7.1 propagation code solves the enhanced Burgers equation along acoustic rays and uses the Schulten flat earth ray tracing equations extended by Lonzaga[9] to include the ray velocity and Doppler shift. A four-ray algorithm approximates the ray tube area during propagation. The atmosphere is assumed to be horizontally stratified and turbulence is neglected. The lateral cutoff rays are determined using an iterative algorithm that launches rays moving outward from undertrack, finding the last ray with hundredths place precision to reach the ground without turning upward, and then moving back toward the carpet centerline by 0.5°. This ray is used as the cutoff ray and results in underprediction of the carpet width.

Fifty-two sonic thumps from a simulated X-59 flight were propagated using the mean aircraft heading and the measured atmospheric profile that corresponded to each low-boom dive from the QSF18 test. The X-59 trajectories were modeled as steady, level supersonic cruise (constant Mach number, constant heading, and zero flight path angle) and not supersonic dives. Use of the mean heading from each F-18 pass as the heading for the X-59 trajectory results in carpets that are approximately perpendicular to the coastline of Galveston, TX. For each propagation simulation, acoustic rays were emitted from undertrack to the predicted lateral cutoff rays at 2° azimuthal increments. A ground reflection factor of 1.9 was applied to the ground waveforms. The PL of the ground waveform at each azimuthal angle was computed. The carpet width for each simulation run was also computed, where carpet width is defined as the flight-track perpendicular distance between the predicted lateral cutoff ray landing positions. A limitation of this study is that other choices for X-59 heading would produce different carpet widths and booms of differing offtrack PL.

B. PROPAGATION RESULTS

Figure 2 shows a histogram of the carpet width of these X-59 boom propagation simulations. The carpet widths ranged from 15 to 40 statute miles (24 to 64 km). Figures 3 and 4 show the PL of the predicted ground waveforms as a function of the acoustic emission angle and offtrack distance, respectively. Offtrack distance is defined as the flight-track perpendicular distance from the landing position of the 0° ray, which is emitted directly beneath the aircraft. The PL for individual carpets is fairly uniform within about ±10 statute miles (±16 km) of the undertrack boom. For the undertrack booms, a PL range of about 8.5 dB was predicted. To determine the source of the PL difference between these booms, a case study was completed that compares various quantities of interest, e.g., ray tube area, frequency spectra, sone spectra, and others (see Section 3), of the highest and lowest PL undertrack booms that were predicted.
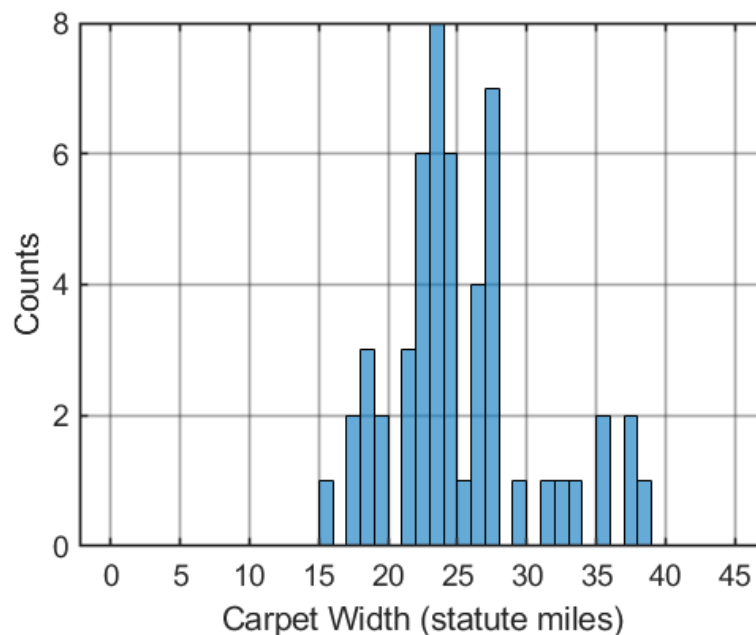

Figure 2. Simulated X-59 sonic boom carpet widths from propagation through balloon-measured atmospheric profiles from QSF18.
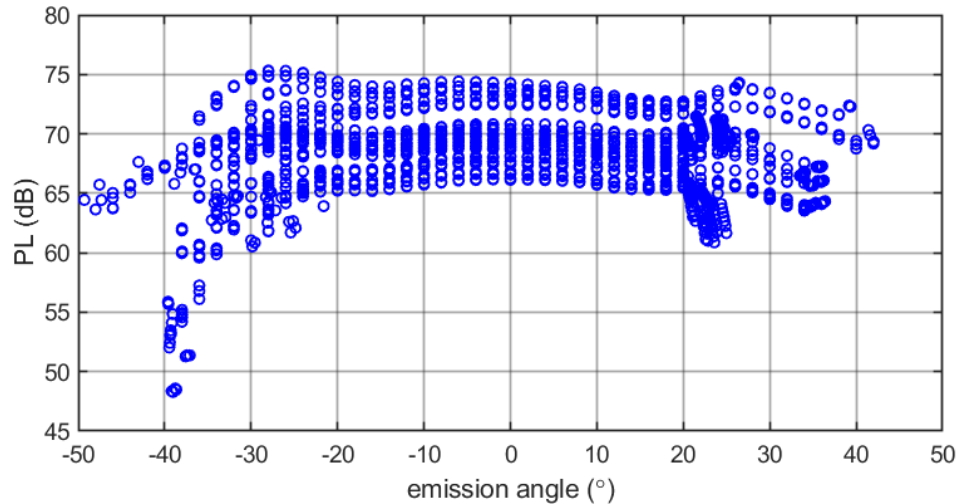
Figure 3. Perceived Level of simulated X-59 ground booms shown as a function of azimuthal emission angle.
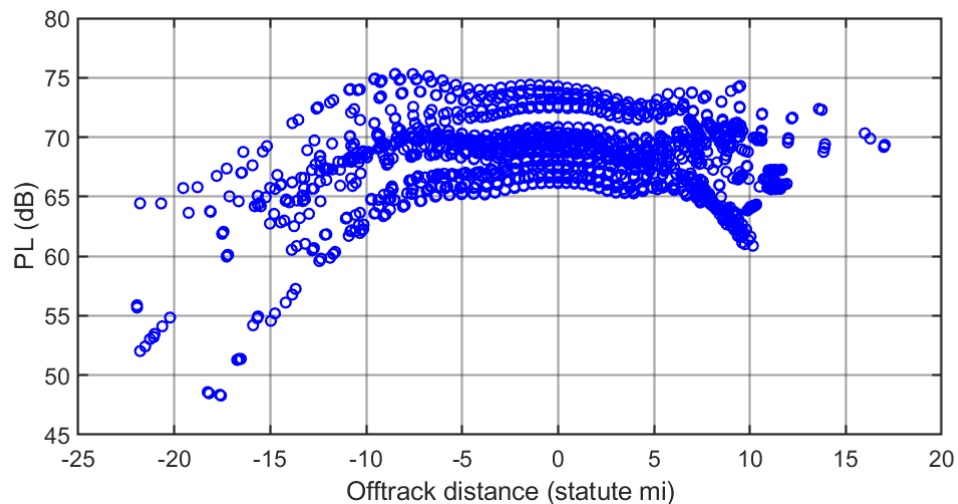

Figure 4. Perceived Level of simulated X-59 ground booms shown as a function of offtrack distance.

3. BOOM COMPARISON CASE STUDY

A. CASE STUDY DESCRIPTION

The PL as a function of offtrack distance for the two booms predicted to have the highest and lowest PL is shown in Figure 5. The difference in aircraft heading between the two cases is small (5.8°). The louder X-59 ground waveform resulted from propagation through the atmospheric profile measured prior to QSF18 flight number 14, which was launched at 12:49 PM local time on November 11, 2018. This will be referred to as the "Loud" atmospheric profile. The quieter boom resulted from propagation through the atmospheric profile measured prior to QSF18 flight number 18, which was launched at 8:37 AM local time on November 14, 2018. This will be referred to as the "Quiet" atmospheric profile.

The atmospheric profiles that produced these booms are shown in Figure 6. The vertical resolution of the balloon data is 1000 ft (304.8 m). The top left plot shows the ambient pressure and includes a black line for the ICAO 7488 standard atmospheric pressure for reference.[10] The top right plot shows the ambient temperature and also includes the ICAO 7488 temperature profile. The bottom left plot shows the east (solid) and north (dash-dotted) vector wind speed. The ICAO standard atmosphere assumes zero wind speed, so it is not explicitly shown. The bottom right plot shows the relative humidity profile and includes the ISO 9613-1:1993 Annex C

humidity profile for reference.[11] The reference atmospheric profile will be referred to as the "Standard" atmospheric profile.
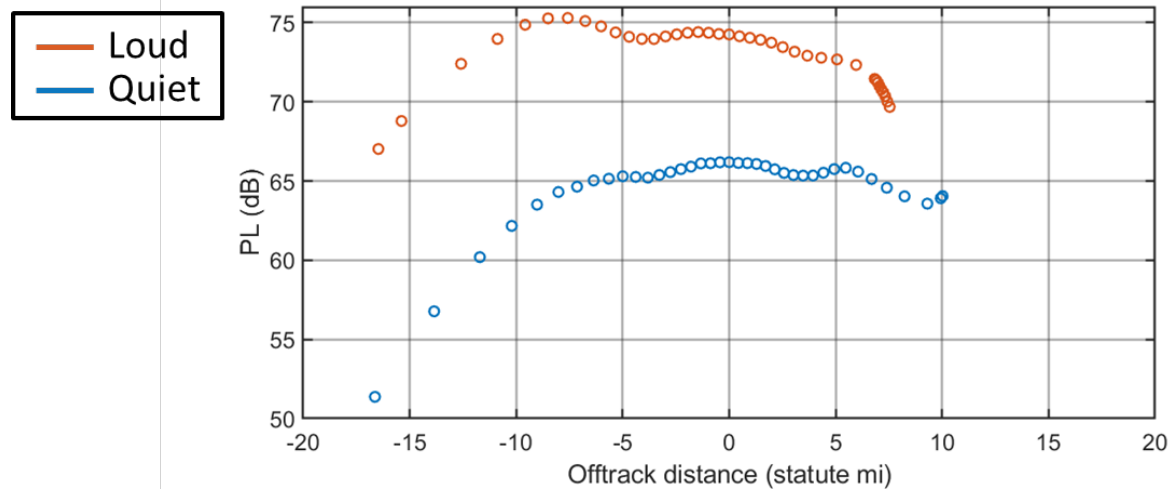

Figure 5. Cross-carpet Perceived Level of the simulation cases resulting in the loudest and quietest undertrack X-59 booms in this dataset.
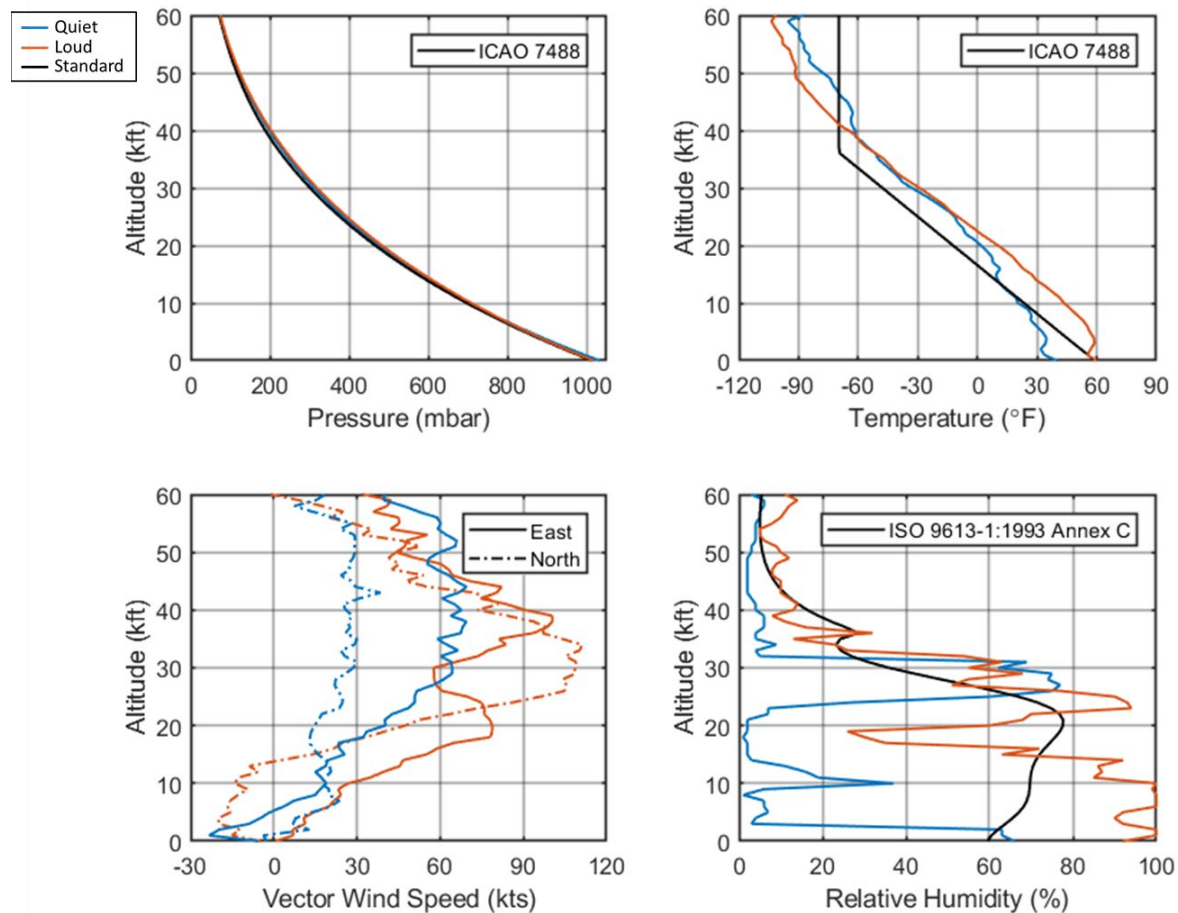

Figure 6. Measured atmospheric profiles for the cases that produced the loudest (red) and quietest (blue) booms.

A case study was completed to probe quantities of interest during propagation and determine the causes of the PL difference between the loudest and quietest undertrack simulated X-59 sonic thumps. Quantities of interest during propagation include the individual waveforms as well as their PL, ray tube area, maximum overpressure, rise time, ray path length, and sone spectra. Absorption curves as a function of frequency are also presented at various altitudes during propagation.

B. CASE STUDY RESULTS

I. WAVEFORM VISUALIZATION DURING PROPAGATION

During propagation, waveforms from the undertrack ray were extracted and compared at every 1000 ft (304.8 m) of altitude. These waveforms are shown in Animation 1 (the animations in this work are available online).[12] The animation is a useful visual aid that offers insight into the waveform evolution from a complicated nearfield to a shaped low-boom at the ground. The top plot in the animation shows the same data as the bottom plot, but at a different pressure scale. The text at the top of the plots shows the altitude of the extracted waveforms and the difference in PL between the red and blue waveforms (i.e., Loud boom PL minus the Quiet boom PL). The waveforms have a 1.9x "ground reflection" factor applied as if the waveform were reaching the ground at the given altitude so that the ground PL can be compared to the aloft PL.

Stepping through Animation 1, the appearance of the waveforms at the beginning of propagation is complicated and contains many shocks. From the flight altitude to about 40,000 ft (12,192 m) above ground, the amplitude quickly drops as geometrical spreading dominates. Then between about 30,000 and 24,000 ft (9,144 and 7,315 m), the shocks present at the front portion of the waveforms are absorbed, resulting in a somewhat sinusoidal waveform shape. Between about 15,000 ft (4,572 m) and the ground, the rear portion of the Quiet waveform becomes more rounded compared to the Loud waveform. While visual comparison can be informative, it may oversimplify the audibility of the booms.
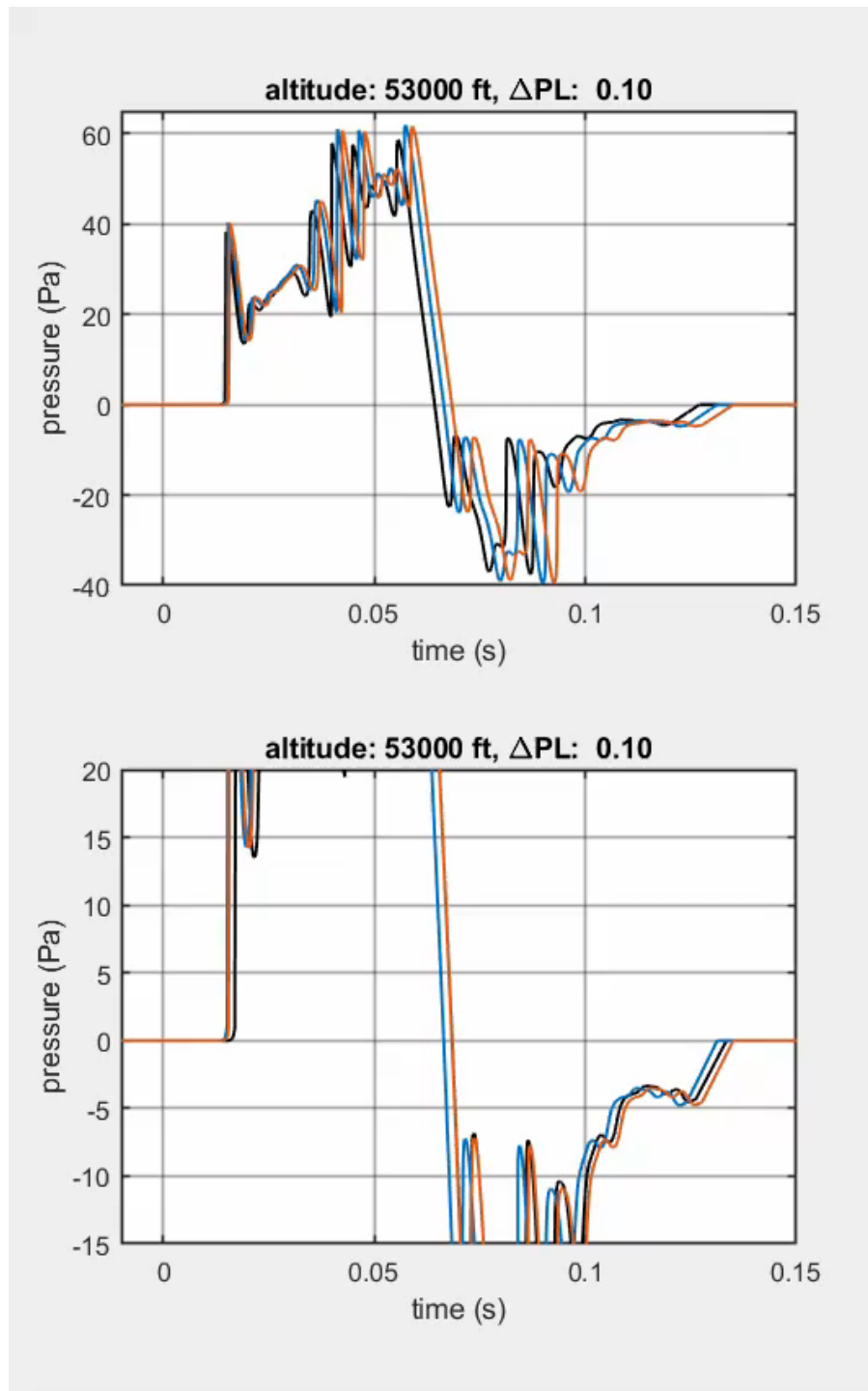
Animation 1 ([see MPEG4 file](#)). Waveforms of the Loud (red), Quiet (blue), and Standard (black) X-59 undertrack booms extracted during propagation.

II. PROBING QUANTITIES OF INTEREST DURING PROPAGATION

Other quantities related to the boom characteristics were computed at 1000-ft (304.8-m) intervals for the Loud, Quiet, and Standard atmosphere. Figure 7a shows the PL for the waveforms as a function of altitude. Geometrical spreading dominates from the flight altitude to about 30,000 ft (9,144 m). Then the rate of PL reduction increases as the shocks are absorbed between 30,000 and 24,000 ft (9,144 and 7,315 m) for the Loud and Quiet atmospheres. For the Standard atmosphere, the rapid PL reduction starts at a lower altitude, at 25,000 ft (7,620 m). Below 24,000 ft, the PL of the Loud and Quiet waveforms begins to diverge. Between 24,000 and

13,000 ft (7,315 and 3,962 m), the boom propagating through the Quiet atmosphere actually has a greater PL than the boom propagating through the Loud atmosphere. Finally, there is a rapid decrease in PL for the Quiet boom between about 15,000 ft (4,572 m) and the ground. It is notable that PL reduction in this altitude range is ultimately responsible for the PL difference predicted at the ground.
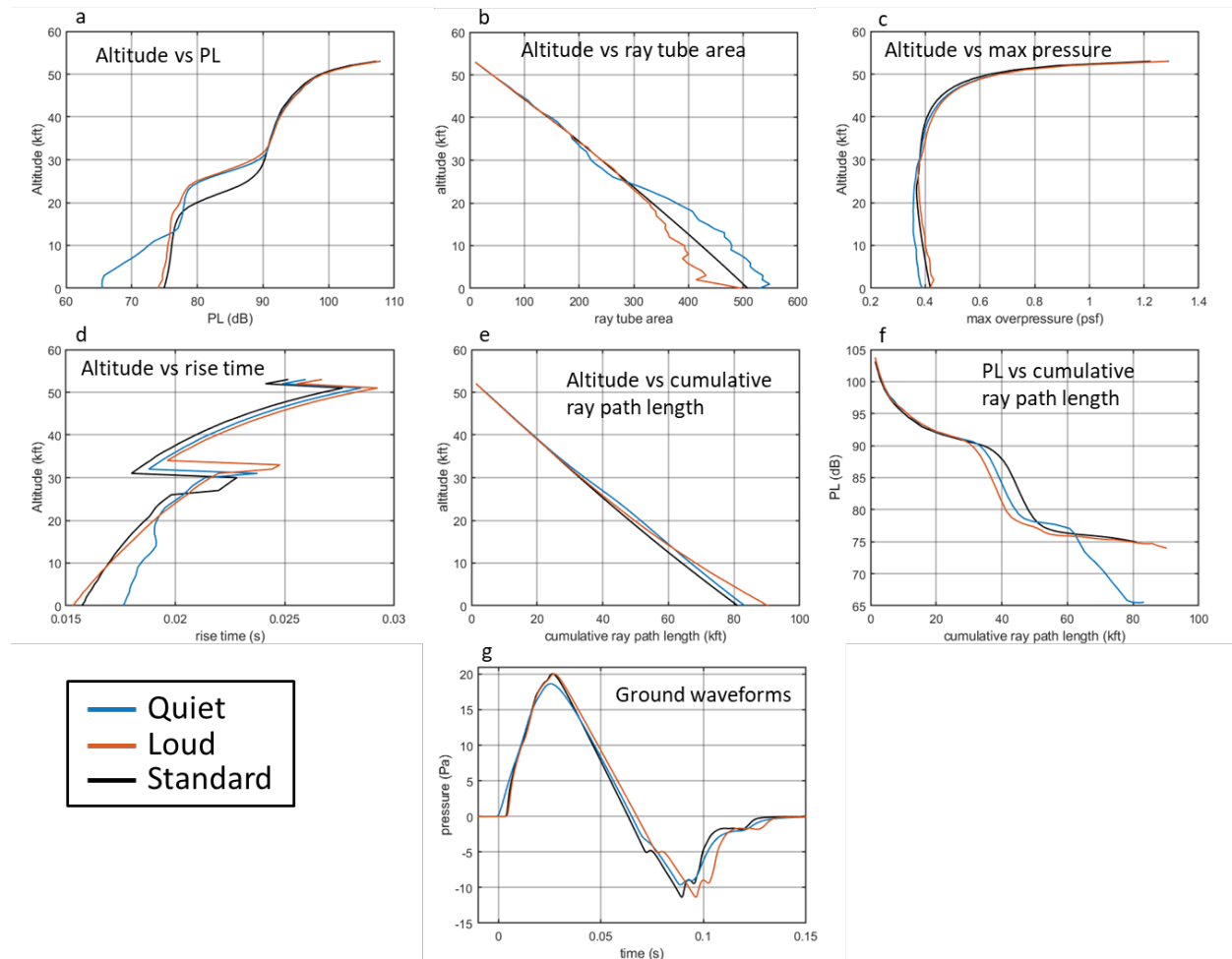

Figure 7. Quantities of interest during propagation of X-59 boom through Loud (red), Quiet (blue), and Standard (black) atmospheres.

Figure 7b compares the ray tube area[13] of the booms throughout propagation. The ray tube areas are nearly equivalent until around 25,000 ft (7,620 m). Then, between about 25,000 and 10,000 ft (7,620 and 3,048 m), the Quiet boom's ray tube area begins to increase in value at a faster rate than the Loud boom. Below 10,000 ft (3,048 m), the ray tube areas increase at about the same rate until near the ground. The Loud boom's ray tube area quickly increases due to a sound speed inversion while the Quiet boom's ray tube area decreases somewhat. The Quiet boom has a larger ray tube area than the Loud boom at the ground, which one may expect because its acoustic pressure has spread to a larger surface. The Standard boom's ray tube area is between the Loud and Quiet booms.

Figure 7c compares the maximum overpressure during propagation. The rapid amplitude reduction from geometrical spreading is apparent near the flight altitude, and the effect begins to level off at about 40,000 ft (12,192 m), which is 14,000 ft (4,267 m) below the flight level. There is a slight increase in overpressure as the waveforms approach the ground, similar to that presented in Figure 4 of Reference 14. The overpressures are nearly equivalent until the 25,000 ft (7,620 m) altitude, which is also where the ray tube areas diverge. The Quiet boom's larger ray tube area results in lower maximum overpressure.

Figure 7d shows the rise time of the waveforms during propagation. The rise time is defined as the duration for the front portion of the waveform to increase from 10% to 90% of the peak pressure amplitude. The effect

of nonlinear steepening is apparent in the curvature of the individual lines. As the waveform steepens, the rise time gradually decreases. The Quiet waveform has a longer rise time at the ground.

There are two regions of rapid rise time increases at 51,000 ft and about 32,000 ft (15,545 m and about 9,754 m). These are due to the complicated waveforms shock structures. The explanation for the rapid increase in rise time at these altitudes is illustrated in Figure 8, which shows the location of the peak pressure, 90% peak pressure, and 10% peak pressure for the Loud boom at 52,000 and 51,000 ft (15,850 and 15,545 m). Two arrows point to two different shock structures. Comparing the left and right plot, the 90% peak pressure location moves between the two different shock structures. The 90% peak pressure location moves from one shock structure at 52,000 ft (15,850 m) to a shock that is closer to the peak pressure location at 51,000 ft (15,545 m). This results in a rapid increase in the calculated rise time. The same explanation is applicable for the rapid increase in rise time around 32,000 ft (9,754 m). Beneath this altitude, the shock structures have become rounded enough that this effect does not repeat.
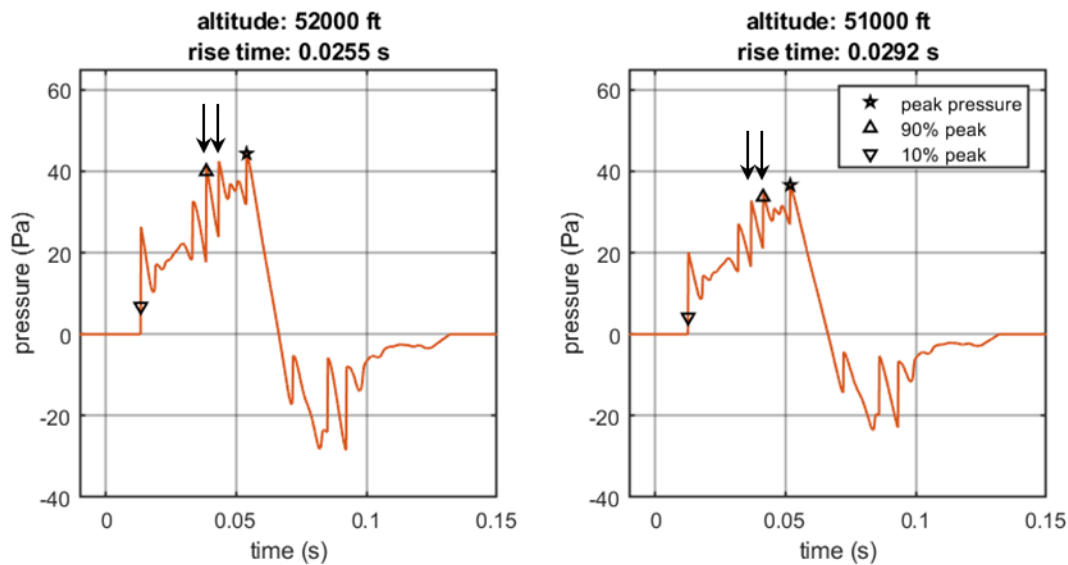

Figure 8. Rapid increase in calculated rise time between waveforms at 52,000 and 51,000 ft resulting from the 90% peak pressure location moving between shock structures.

Figure 7e shows the cumulative ray path length of the booms as they move toward the ground, and Figure 7f shows how the PL changes with cumulative ray path length. The Quiet boom travels a shorter distance in total than the Loud boom by several thousand feet. The Standard boom travels the shortest distance. A shorter total ray path has less opportunity for shaped booms to experience loudness increases due to waveform steepening. However, a shorter ray path also has less opportunity for spreading and absorption to reduce the loudness.

Figure 7g shows the ground waveforms of the booms. The Quiet boom has a lower peak amplitude and a more gradual initial rise. The rear of the Quiet boom also appears more rounded than the Loud boom. These factors likely contribute to its lower PL.

III. ABSORPTION SPECTRA VARIATION DURING PROPAGATION

Absorption plays an important role in reducing the loudness of low booms. Animation 2 shows the absorption coefficient as a function of frequency during propagation.[15,16] Key frames of the animation have been extracted at 10,000 ft (3,048 m) increments from 50,000 to 10,000 ft and at 5,000 ft (15,240 to 3,048 m, and at 1,524 m) in Figure 9. These correspond to altitudes of notable changes in the rate of change in PL aloft (see Figure 7a). The absorption curves are very similar for all three atmospheric profiles for the 50,000 ft, 40,000 ft, and 30,000 ft (15,240 m, 12,192 m, and 9,144 m) altitudes. Relaxation of oxygen is responsible for absorption in the audible range at and below 30,000 ft (9,144 m), and there is substantial PL reduction for the next 8,000 ft (2,438 m) of propagation as the shocks are rounded. The humidity profiles first begin to substantially diverge below 25,000 ft (7,620 m) or so, and the absorption curves reflect this. At 20,000 ft (6,096 m) there is more reduction in the 1 kHz band for the Loud atmosphere. By 10,000 ft (3,048 m) this trend has reversed, and most of the audible content above 1 kHz has been absorbed for both the Loud and Quiet booms. From 10,000 ft (3,048

m) to the ground, the Quiet atmosphere has more absorption below 1 kHz for most of the rest of propagation, resulting in a lower PL X-59 boom at the ground.
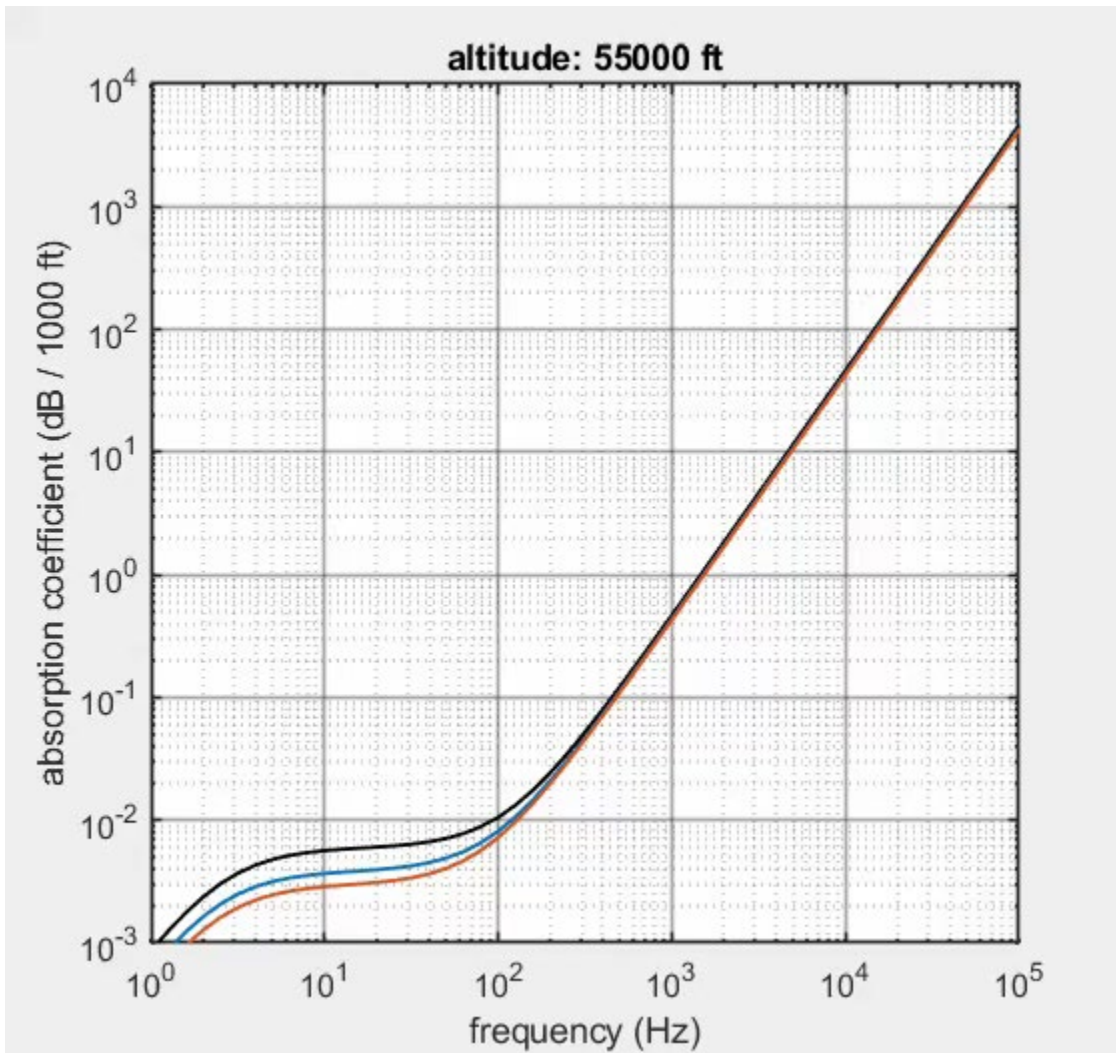
Animation 2 (see MPEG4 file). Absorption as a function of frequency for the Loud (red), Quiet (blue), and Standard (black) atmospheric profiles.
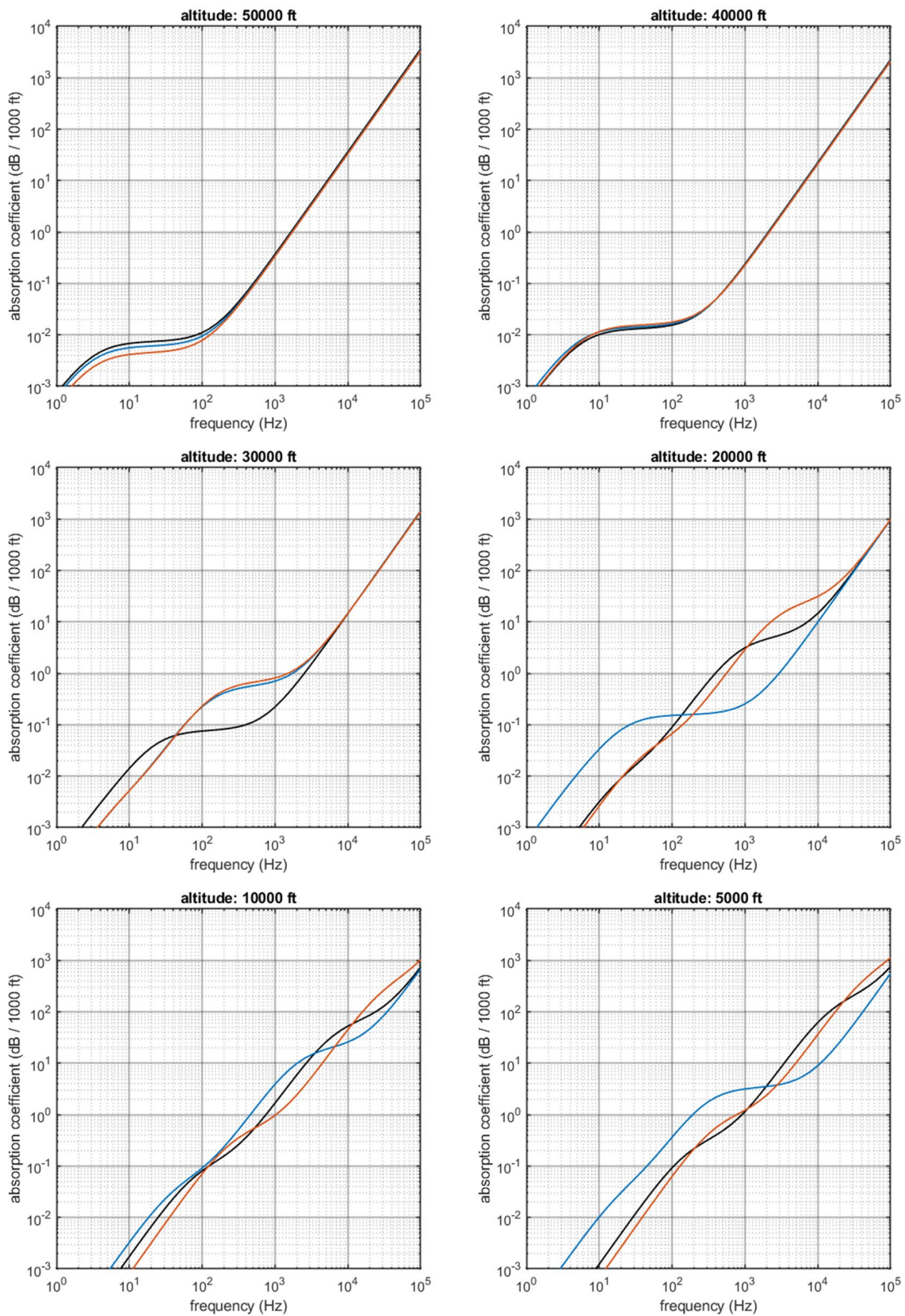
Figure 9. Absorption as a function of frequency for select altitudes for the Loud (red), Quiet (blue), and Standard (black) atmospheric profiles. Intermediate altitudes are shown in Animation 3.

IV. SONE SPECTRA DURING PROPAGATION

An intermediate step in calculating the PL of a waveform is computing the loudness in sones of 1/3rd octave bands. It is informative to evaluate the sone spectra of the extracted waveforms as they propagate to the ground to show which frequency bands are the strongest contributors to the PL metric.

Animation 3 shows these sone values and other quantities as the waveforms move through the atmospheres. The first column of plots is a repeat of Animation 1, which shows the two X-59 waveforms at various altitudes and the difference in PL between the two waveforms. The second column of plots shows information on the sone values of the waveforms. The top plot shows the sone spectra, and the bottom plot shows the difference in sone value from the previous 1000 ft (304.8 m) of altitude normalized to the maximum sone value shown on the top plot. A negative Δsone value for a frequency band indicates that audible sound was absorbed during the 1000 ft (304.8 m) propagation step. The third column of plots shows the PL and ray tube area of the waveforms with a dashed horizontal line showing the altitude of the current animation frame. The rightmost plot shows the relative humidity profiles.

Initially, the entire sone spectra decrease rapidly as the pressure amplitude decreases due to the geometrical spreading near the aircraft. This is followed by substantial high frequency sone loss as the shocks are absorbed starting at around 30,000 ft (9,144 m). By 24,000 ft (7,315 m) the sone spectrum above 1 kHz and the PL for the Quiet boom is actually greater than the Loud boom. The PL of the Quiet boom at the ground remains louder aloft for more than 10,000 ft (3,048 m) despite its ray tube area increasing relative to the Loud boom. By 12,000 ft (3,658 m), the Loud and Quiet booms have nearly equivalent PL even though their sone spectra are different. Below 12,000 ft (3,658 m), the sone and PL of the Quiet boom decreases substantially. The relative humidity for the Quiet atmosphere is much lower for this altitude range. The lower humidity results in increased absorption at and below 1 kHz where there is still audible content in the signals. The band with the maximum sone value at the ground is 100 Hz for the Quiet boom and 125 Hz for the Loud and Standard booms. The Quiet boom has experienced more absorption in these bands during propagation, which reduces its PL.
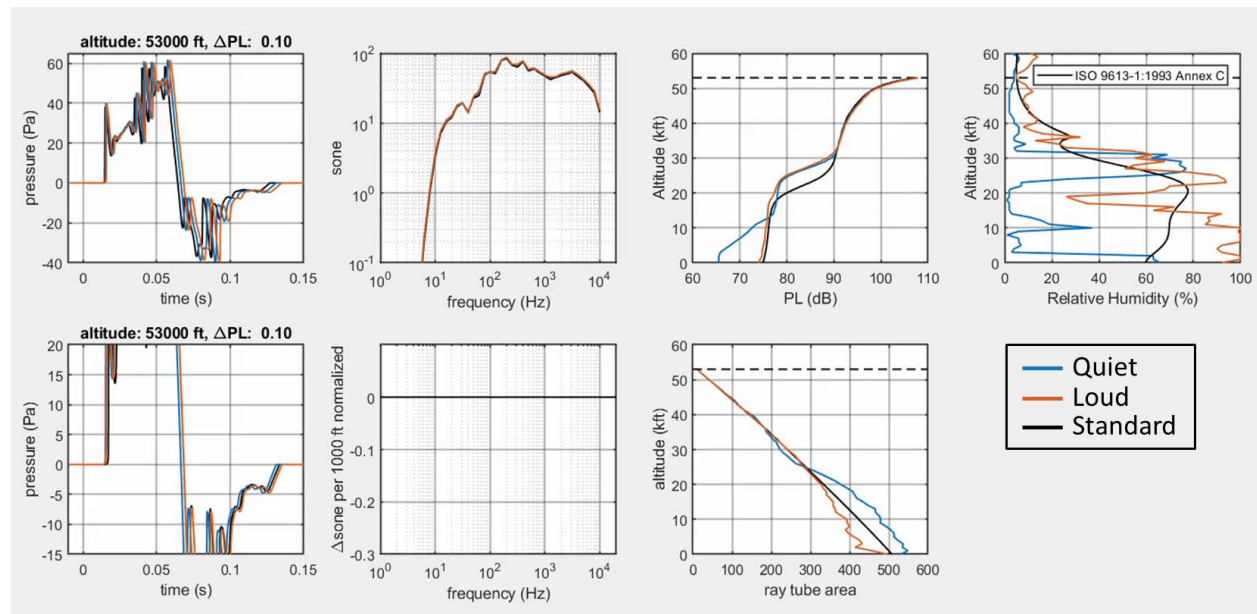
Animation 3 ([see MPEG4 file](#)). Reduction in sone during propagation compared to the waveforms, PL, ray tube area, and relative humidity profile for Loud (red), Quiet (blue), and Standard (black) booms.

V. SONE REDUCTION DURING PROPAGATION

The absorption curves in Animation 2 and Figure 9 apply to the sound pressure levels, which do not map one-to-one to sone values. Figure 10 shows the change in sone per 1000 ft (304.8 m) for the Quiet and Loud booms. The colored curves correspond to various 1/3rd octave band frequencies. The curves show sizeable sone loss due to geometrical spreading from the flight altitude to about 35,000 ft (10,668 m). Then there is a region of sone loss as the audible content from the shocks is absorbed between 30,000 ft and 20,000 ft (9,144 and 6,096 m). The primary difference in sone reduction for the Quiet and Loud atmospheres occurs in the altitude range

below 15,000 ft (4,572 m). For the Quiet boom, there is additional absorption of sound in the 1 kHz band from 15,000 to 10,000 ft (4,572 and 3,048 m) and additional absorption of sound at the 100 Hz band between 10,000 ft and about 3,000 ft (3,048 and 914.4 m) that is not present for the Loud boom.
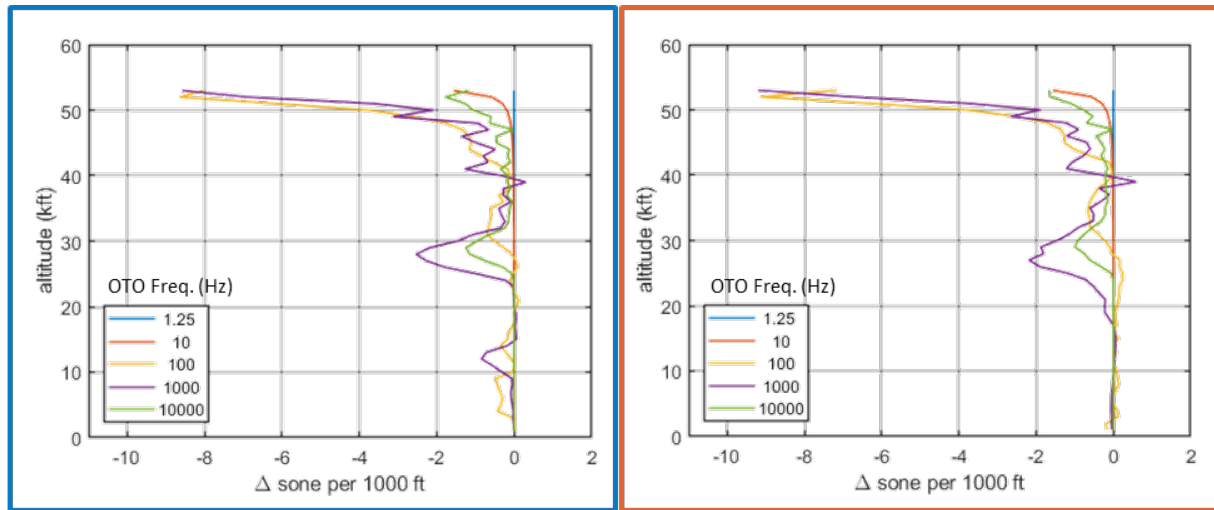

Figure 10. Changes in sone values per 1000 ft for various 1/3ʳᵈ octave band frequencies for the Quiet (left) and Loud (right) simulated X-59 sonic thumps.

C.   CASE STUDY CONCLUSION

The quantities of interest that were probed in this case study provide physical insight into attenuation mechanisms during the propagation of shaped sonic booms. The extracted waveforms in Animation 1 show the rapid amplitude decay from spreading as well as nonlinear steepening. They also show the shocks being rounded due to atmospheric absorption. The rise-time curves show a challenge of using this metric on shaped booms since their shock structures can be more complicated than N-wave booms. Another notable aspect is the reminder that absorption depends on humidity, temperature, and pressure (and not for humidity simply to be low). As a demonstration of this, the humidity is above 50% at the altitude where the shocks are rapidly absorbed (~30,000 ft (9,144 m)). Near the ground, it is true that the absorption rates are typically higher for lower humidity.

The primary region where the PL diverged between the Quiet and Loud simulated X-59 booms in QSF18 atmospheric profiles was below 15,000 ft (4,572 m). In this region, the rate of increase of ray tube area was roughly the same, but the relative humidity profiles differed substantially. As a result, the Quiet boom experienced higher rates of absorption in this region. The sizable difference in PL due only to the macroscopic atmospheric effects illustrates a challenge for planning X-59 low-boom community noise surveys. The aircraft's condition will need to be adjusted to produce the noise levels that are planned for each pass over the community based on accurate, local atmospheric conditions.

4.   SUMMARY

NASA will soon be using the X-59 as the noise source for low-boom community noise surveys across the USA. In the QSF18 community noise survey, substantial weather variability was observed in measured atmospheric profiles. An X-59 low-boom propagation simulation study was completed using the QSF18 atmospheric profiles as inputs to PCBoom to see how such variability would affect the X-59's design cruise boom carpet. For the same initial X-59 nearfield pressure signature, application of the QSF18 atmospheres resulted in carpets varying from 15 to 40 statute miles wide, and the undertrack booms on the ground had a PL range of 8.5 dB. A case study was completed comparing the two undertrack booms that were predicted to have the greatest difference in PL. Waveforms and other quantities of interest were extracted every 1,000 ft (304.8 m) during propagation. Differences in absorption due to differences in relative humidity below 15,000 ft (4,572 m) were primarily responsible for the observed difference in PL. The Loud boom also had a higher maximum pressure, smaller ray tube area, shorter rise time than the Quiet boom, which contribute to its higher PL. However, it also had a longer propagation path than the Quiet boom, which one might not expect.

The X-59 community noise surveys will likely be designed to expose communities to specific boom levels on a predetermined schedule. This study shows the impact of macroscopic atmospheric effects on low-booms, and that it will be necessary for the X-59 to fly over communities at conditions that differ from the design cruise condition in order to achieve the target boom level on the ground. To achieve this, teams at NASA are developing the Community Low-boom Exposure, Operations, Piloting and Trimming Analyzer (CLEOPATRA), which is a software package that will accept inputs such as the target boom loudness level and state of the atmosphere and output the vehicle state to achieve the target boom level.

ACKNOWLEDGMENTS

REFERENCES

[1] G. Shah, A. Loubeau, and J. Rathsam, "Low-boom Flight Demonstration Mission - Phase 3 Community Testing," *AIAA SciTech Forum,* (2021).

[2] S. S. Stevens, "Perceived Level of Noise by Mark VII and Decibels (*E*)," *J. Acoust. Soc. Am.* **51**, 575-601 (1972). doi.org/10.1121/1.1912880

[3] K. P. Shepherd and B. M. Sullivan, "A loudness calculation procedure applied to shaped sonic booms," *NASA Technical Report* NASA/TP-3134, (1991). ntrs.nasa.gov/citations/19920002547

[4] W. J. Doebler, S. R. Wilson, A. Loubeau, and V. W. Sparrow, "Five-year simulation study of NASA's X-59 low-boom carpets across the contiguous United States of America," *e-Forum Acusticum 2020*.

[5] J. A. Page, *et al.*, "Quiet Supersonic Flights 2018 (QSF18) Test: Galveston, Texas Risk Reduction for Future Community Testing with a Low-Boom Flight Demonstration Vehicle," *NASA Contractor Report* NASA/CR–2020-220589/Volume I, (2020). ntrs.nasa.gov/citations/20200003223

[6] E. Haering, L. Cliatt, T. Bunce, T. Gabrielson, V. Sparrow, and L. Locey, "Initial results from the variable intensity sonic boom propagation database," *14th AIAA/CEAS Aeroacoustics Conference (29th AIAA Aeroacoustics Conference)*, AIAA 2008-3034, May 2008. doi.org/10.2514/6.2008-3034

[7] S. K. Rallabhandi and A. Loubeau, "Summary of propagation cases of the Third AIAA Sonic Boom Prediction Workshop," *AIAA SciTech Forum*, (2021). doi.org/10.2514/6.2021-0229

[8] J. A. Page, *et al.*, *PCBoom Version 6.6 Technical Reference and User Manual*, *Wyle Report* WR 10-10, (2010).

[9] J. B. Lonzaga, "Recent Enhancements to NASA's PCBoom Sonic Boom Propagation Code," *AIAA Aviation Forum* (2019). doi.org/10.2514/6.2019-3386

[10] *Manual of the ICAO Standard Atmosphere Extended to 80 kilometres (262 500 feet).* International Civil Aviation Organization ICAO 7488, (1993).

[11] *Acoustics — Attenuation of sound during propagation outdoors — Part 1: Calculation of the absorption of sound by the atmosphere*, ISO Standard 9613-1:1993, (1993).

[12] Animations in this work are available for download at https://stabserv.larc.nasa.gov/cst/.

[13] J. A. Page, *et al.*, "Section 3.3.2 Ray Paths" in *PCBoom Version 6.6 Technical Reference and User Manual*, *Wyle Report* WR 10-10, p. 23, (2010).

[14] C. L. Thomas, "Extrapolation of Wind-Tunnel Sonic Boom Signatures Without Use of a Whitham *F*-Function," in *Third Conference on Sonic Boom Research* NASA/SP-255, 205-217 (1971). ntrs.nasa.gov/citations/19710018887

[15] H. E. Bass, *et al.*, "Atmospheric absorption of sound: further developments," *J. Acoust. Soc. Am.* **97**, 680-683 (1995). doi.org/10.1121/1.412989

[16] H. E. Bass, *et al.*, "Erratum: Atmospheric absorption of sound: further developments [*J. Acoust. Soc. Am.* **97**, 680–683 (1995)]," *J. Acoust. Soc. Am.* **99**, 1259 (1996). doi.org/10.1121/1.415223